

**NASA Technical Memorandum** 104181  
**AVSCOM Technical Report** 91-B-018

IN-27  
75765  
P-17

**DELAMINATION BEHAVIOR OF QUASI-ISOTROPIC  
GRAPHITE EPOXY LAMINATES SUBJECTED TO  
TENSION AND TORSION LOADS**

J. A. Hinkley and T. K. O'Brien

Paper Presented at the American Helicopter Society Specialists' Meeting  
Williamsburg, Virginia, October 29, 1991

(NASA-TM-104181) DELAMINATION BEHAVIOR OF  
QUASI-ISOTROPIC GRAPHITE EPOXY LAMINATES  
SUBJECTED TO TENSION AND TORSION LOADS  
(NASA) 17 p

N92-22624

CSCL 11B

Unclass  
0075765

63/27

January 1992

**NASA**

National Aeronautics and  
Space Administration

Langley Research Center  
Hampton, Virginia 23665-5225



US ARMY  
AVIATION  
SYSTEMS COMMAND  
AVIATION R&T ACTIVITY

Vertical text on the right edge of the page, possibly a page number or margin indicator.

# Delamination Behavior of Quasi-Isotropic Graphite Epoxy Laminates Subjected to Tension and Torsion Loads

J. A. Hinkley and T. K. O'Brien

## Abstract

Sixteen and thirty-two ply quasi-isotropic laminates fabricated from AS4/3501-6 were subjected to pure tension, pure torsion, simultaneous tension and torsion, and torsion fatigue. Layups tested were  $[45_n/-45_n/0_n/90_n]_s$ , with  $n=2$  or  $4$ . A torsion damage pattern consisting of a localized matrix crack and delaminations was characterized, and the measured torsional stiffnesses were compared with calculated values. It was found that a combination of tension and torsion led to failure at smaller loads than either type of deformation acting alone. Further work is required to determine the exact form of the failure criterion.

## Introduction

The delamination of multidirectional composite laminates subjected to tensile loads is fairly well understood. The effects of lay-up, moisture, thermal residual stresses, and resin toughness have been described.<sup>1,2</sup> In some structural applications, including helicopter rotors, composites are subjected to a combination of tension and torsion. In this report the damage induced in quasi-isotropic graphite/epoxy laminates subjected to pure torsion and combined tension and torsion loads will be described and contrasted to the damage observed in these same laminates when subjected to pure tension loading.

## Experimental Procedures

Sixteen and thirty-two ply quasi-isotropic laminate plates with a  $[45_n/-45_n/0_n/90_n]_s$  layup (where  $n=2$  and  $4$ ) were fabricated from Hercules AS4/3501-6 graphite/epoxy prepreg using the manufacturer's recommended autoclave cycle. Specimens 1" wide and 5" or 10" long were cut from the plates.

Tension-only tests were run in stroke control, using a clip gauge to monitor strain. Tension/torsion testing was performed using a servohydraulic test frame equipped with hydraulic wedge grips. Torsion tests and combined tension/torsion tests were run in rotary stroke control and axial load control. Angles of twist were determined by the rotary transducer mounted on the hydraulic actuator. Axial load was monitored and verified to be constant and independent of the angle of twist. Static

tests were run at a rate of 0.125 degrees/sec; fatigue experiments were performed with a load ratio of  $R=0.10$  under sine-wave loading at 5 Hz. Specimen edges were coated with water-based typewriter correction fluid to aid in visual detection of the onset of damage. Critical strains and critical angles of twist were recorded when delamination occurred. After testing, some specimens were treated with a dye-penetrant that is opaque to x-rays, then x-rayed. Specimen edges were later polished for photomicroscopy.

### Experimental Results

Critical delamination strains, critical loads, and moduli obtained from static tests in pure tension are summarized in Table I. Failures in this type of tensile specimen have been described previously.<sup>1</sup> Delaminations form in the 0/90 interface, jumping through the 90° plies to the symmetric 90/0 interface randomly along the entire length of the free edge between the grips.

The data for pure torsion are shown in Table II. The critical normalized angle of twist for delamination,  $\theta/L$ , is relatively independent of the gauge length but decreases with increasing specimen thickness.

The damage pattern observed on the edges of the 16 and 32 ply specimens is shown in Fig. 1. On each edge, one oblique crack in the central 90° plies has a pair of delaminations growing at either end of it in opposite directions. This "primary" crack is presumed to be the point where the delaminations initiated. A schematic of the characteristic failure mode is shown in Fig. 2. The delaminated areas show up quite clearly in the dye penetrant enhanced radiographs. The hourglass-shaped shadow in Fig. 3 marks the boundaries of the edge delaminations. Furthermore, both the x-ray and optical microscopy (Fig. 4) reveal the primary crack as well as other secondary matrix cracks that develop in the 90° plies.

The effects of combined tension/torsion may be studied using the same type of specimen. To do this, a constant axial load, equal to approximately 1/2 the failure load in pure tension, was applied to the specimen as the torsion load was introduced. Figure 5 shows the delamination onset data from the pure tension, pure torsion, and combined tension and torsion tests, with the axial strain shown on the ordinate and the normalized angle of twist shown on the abscissa. Curves are faired through the maximum and minimum values to bound the data. Figure 6 shows the delamination data in terms of the axial load and torque.

Based on the elasticity solution for the torsion of a rectangular prismatic bar,<sup>4</sup> the maximum shear stress should occur at the midplane of the laminate thickness. Because of the laminated nature of composites, however, deviations from pure shear may occur near the edge. The matrix

crack visible in Fig. 4a. makes an angle of approximately  $50^\circ$  with the specimen face. Among all the specimens tested in pure torsion this angle ranged from  $37^\circ$  to  $65^\circ$ , with a mean of  $51^\circ$ . The corresponding cracks in a tension specimen lie at  $90^\circ$  (perpendicular to the tensile direction.) It was therefore anticipated that as greater proportions of tension loading were added in tension-torsion tests, the angle would increase toward  $90^\circ$ . The data from all the micrographs examined are collected in Table III. As had been expected, delaminations did form at a smaller angle of twist in these combined loading specimens than they had in specimens tested in pure torsion. However, the matrix cracks made an average angle of  $52^\circ$ , only a slight deviation from the pure torsion result.

Preliminary torsion fatigue data are displayed in Fig. 7. The logarithm of the number of cycles to delamination onset increases steadily with decreasing strain. No critical strain threshold (leveling out of the curve) is apparent out to  $10^6$  cycles.

#### Estimation of Torsional Rigidity

From strength of materials<sup>5</sup>, the torsional rigidity of an isotropic prismatic bar is defined as the product of the shear modulus,  $G$ , and the polar moment of inertia,  $J$ , and is determined as

$$JG = \frac{TL}{\theta} \quad (1)$$

where  $T$  is the applied torque,  $L$  is the length of the bar, and  $\theta$  is the angular deformation of the bar measured in radians. In plate theory<sup>6</sup>, the torque is given by

$$T = M_{xy} w \quad (2)$$

where  $M_{xy}$  is the twisting moment per unit width,  $w$ , and the twisting curvature is given by

$$\kappa_{xy} = \frac{\theta}{L} \quad (3)$$

Substituting Eq.(2) and Eq.(3) into Eq.(1) yields

$$JG = \frac{TL}{\theta} = \frac{M_{xy}w}{\kappa_{xy}} \quad (4)$$

In laminated plate theory<sup>7</sup>, the twisting curvature may be related to the twisting moment by the following

$$\kappa_{xy} = D_{66}^{-1} M_{xy} \quad (5)$$

where  $D_{66}^{-1}$  represents the last term in the inverse bending stiffness matrix. Substituting Eq.(5) into Eq.(4) yields an estimate for the torsional rigidity of a composite plate as

$$JG = \frac{TL}{\theta} = \frac{w}{D_{66}^{-1}} \quad (6)$$

Therefore, for a composite laminate of known width, lamina properties, stacking sequence, and ply thicknesses, we can use Eq.(6) to estimate the torsional rigidity of the plate. Equation (5) assumes that a torque is applied to all four sides of the laminated plate. In our study, however, the two longitudinal sides are stress free. Hence, laminated plate theory will underestimate the torsional rigidity because of the discrepancy between the actual boundary conditions and those assumed implicitly in Eq.(6).

A more accurate estimate of the torsional rigidity for these quasi-isotropic plates may be obtained from the elasticity solution for an isotropic prismatic bar of rectangular cross section loaded in torsion at the ends.<sup>4</sup> The torsional rigidity from this solution may be expressed as<sup>8</sup>

$$JG = \frac{TL}{\theta} = wt^3G\beta \quad (7)$$

where

$$\beta = \frac{1}{3} \left( 1 - 0.63 \frac{t}{w} \right)$$

and  $t$  is the plate thickness and  $G$  is the shear modulus. This solution now incorporates the appropriate boundary conditions. However, the laminate is assumed to be isotropic. The quasiisotropic composite laminate is isotropic in the plane of the laminate, but the through-thickness properties are anisotropic. Hence,  $G_{xy} = G_{xz}$ , but  $G_{xy}$  is not equal to  $G_{yz}$ . Therefore, the elasticity solution for an orthotropic prismatic bar of rectangular cross section loaded in torsion at the ends<sup>9</sup> may be more appropriate. The torsional rigidity from this solution may be expressed as<sup>8</sup>

$$JG = \frac{TL_z}{\theta} = wt^3 G_{xz} \beta(c) \quad (8)$$

where

$$\beta = \frac{32c^2}{\pi^4} \sum_{n=1,3,5..}^{\infty} \frac{1}{n^4} \left( 1 - \frac{2c}{n\pi} \tanh \frac{n\pi}{2c} \right)$$

and

$$c = \frac{w}{t} \sqrt{\frac{G_{yz}}{G_{xz}}}$$

The properties in table V were assumed in order to calculate  $G_{xy}$  from laminated plate theory as

$$G_{xy} = \frac{1}{A_{66}^{-1}} \quad (9)$$

where  $A_{66}^{-1}$  is the last diagonal term in the inverse extensional stiffness matrix. To determine the torsional rigidity,  $G$  was set equal to  $G_{xy}$  in Eq.(7) and  $G_{xy} = G_{xz}$  in Eq.(8). Two different values of  $G_{yz}$ , the out-of-plane shear modulus, were reported for AS4/3501-6 in Reference.8. The value of  $G_{yz}$  measured for an orthotropic  $[0/45/-45/0]_{2s}$  laminate was less than  $G_{yz}$  measured for a unidirectional laminate, illustrating the anisotropic nature of this property. No value was available in the literature for a quasi-isotropic laminate similar to the ones tested in the present study, so both values of  $G_{yz}$  from Table 2 of Ref.[8] were used in Eq.(8) to predict the torsional rigidity of a quasi-isotropic laminate. Only the first 5 terms ( $n = 1,3,5,7,9$ ) in the series expression for  $\beta$  in Eq.(8) were required for this series to reach a converged value.

Figure 8 shows the experimental values of torsional rigidity measured in this study (EXP) as well as calculated values. The bars labeled LPT were estimated from laminated plate theory using Eq.(6). The isotropic elasticity results from Eq.7 are designated ISO and the two sets of orthotropic elasticity results from Eq. 8 are designated ORTHO ELAS. Comparing these results, we see that the torsional rigidity estimated from laminated plate theory using Eq.(6) is significantly lower than the experimental values due to the error in implicit boundary conditions noted previously. The measured torsional rigidity may not agree precisely with Eqs.(7) and (8) because experimentally the angle of twist,  $\theta$ , was measured using the angular deflection of the lower grip relative to the upper grip. The assumption of uniform warping used to develop these solutions is violated unless  $\theta$  is measured between two points on the specimen away

from the grips. A better measurement of  $\theta$  would be expected to lead to better agreement with the calculation. Nevertheless, the agreement between the experimentally measured torsional rigidity and the calculations from Eqs.(7) and (8) is reasonable.

### Discussion

The effect of combining tension and torsion loads is seen in Fig. 5 and Fig. 6. The combination of torsion and tension results in an earlier delamination failure than would be observed by either loading acting alone. The data generated in this study indicate that a continuous failure criterion may be developed to account for the combination of loads. It is not yet clear what parameter should be used for this criterion or what form the criterion would have. It is desirable to cast the criterion in terms of a generic parameter, one that is independent of structural parameters such as layup, stacking sequence, thickness, gage length, etc. The data in Figures 5 and 6 clearly show a thickness dependence. Hence, critical values of loads (torques) and strains (twist angle per unit length) are structural properties, not generic material properties.

For tension loading, the delamination failure criterion was cast in terms of a critical strain energy release rate,  $G_c$ , assuming an edge delamination geometry<sup>1</sup>. For torsion or combined tension/torsion loading, however, a local delamination model may be needed, similar to a  $G$  solution derived previously for tension<sup>10</sup> because the delamination appears to emanate from a dominant matrix crack and grow in an antisymmetric pattern (Fig.2). The torsional rigidity terms in a local delamination "G" solution for torsion cannot be represented using laminated plate theory, as was done in tension, however, because of the discrepancy in edge boundary conditions between the test specimen loaded at the two ends only and the laminated plate theory assumption of torsion applied to all four sides. Further work is needed to resolve these difficulties.

Other investigators are developing 3D finite element analyses for the interlaminar stresses and strain energy release rates associated with local delamination induced by torsion or combined tension/torsion loading<sup>11</sup>. These models should help explain the local stress states through the 90 degree ply thickness that result in the observed matrix crack angles (Table III). Also, these models will provide benchmark solutions with which to calibrate any simple closed-form models that may be developed for strain energy release rates associated with local delamination induced by torsion or combined tension/torsion loading.



## Conclusions

Based on the experiments conducted in this study, the following conclusions have been reached:

1. For torsion or combined tension/torsion loading, delamination appears to emanate from a dominant matrix crack and grow in an antisymmetric pattern. This pattern is markedly different from the edge delamination pattern observed for tension loading on the same laminate.
2. For pure torsion loading, the angle of the dominant matrix crack with the laminate axis is not simply 45 degrees as anticipated based on the maximum shear obtained from the elasticity solution for a prismatic bar with a rectangular cross section. Furthermore, this crack angle changes very little when tension loading is combined with torsion loading, evidently due to the influence of anisotropy and the free edge.
3. Critical values of loads (torques) and strains (twist angle per unit length) depend on specimen thickness, and hence, are structural properties, not generic material properties.
4. The addition of torsion to tension results in an earlier delamination failure than would be observed under either loading acting alone.
5. Torsional rigidity cannot be represented using laminated plate theory because of the discrepancy in boundary conditions between the test geometry, which involves loading the specimen at the two ends only, and the laminated plate theory assumption of torsion applied to all four sides.

## References

1. O'Brien, T. K., "Mixed-Mode Strain-Energy-Release Rate Effects on Edge Delamination of Composites", in Effects of Defects in Composite Materials, ASTM STP 836, American Society for Testing and Materials, Philadelphia, 1984, pp.125-142.
2. O'Brien, T.K., Raju, I.S. and Garber, D.P. "Residual Thermal and Moisture Influences on the Strain Energy Release Rate Analysis of Edge Delamination", J. Composites Technology and Research vol 8. No. 2, Summer 1986, pp. 37-47.
3. O'Brien, T.K., "Local Delamination in Laminates with Angle Ply Matrix Cracks: Part II, Delamination Fracture Analysis and Fatigue Characterization", NASA TM 104076, June 1991.
4. Timoshenko, S.P. and Goodier, J.N., Theory of Elasticity, 3rd Edition, McGraw-Hill Book Co., Inc., New York, NY, 1951.
5. Popov, E.P., Introduction to Mechanics of Solids, Prentice Hall, Inc., Englewood Cliffs, NJ, 1968.
6. Timoshenko, S.P., and Woinowsky-Krieger, S., Theory of Plates and Shells, 2nd Edition, McGraw-Hill Book Co., Inc., New York, NY, 1959.
7. Jones, R.M., Mechanics of Composite Materials, McGraw Hill, Washington, D.C., 1975.
8. Sumsion, H.T. and Rajapakse, Y.D., "Simple Torsion Test for Shear Modulus Determination," Proceedings of the 2nd International Conference on Composite Materials (ICCM 2), Toronto, April, 1978, pp. 994-1002.
9. Lekhnitski, S.G., Theory of Elasticity of an Anisotropic Elastic Body, Holden-Day, Inc., San Francisco, 1963.
10. O'Brien, T. K., "Analysis of Local Delaminations and Their Influence on Composite Laminate Behavior," in Delamination and Debonding, W.S. Johnson, ed. ASTM STP 876, American Society for Testing and Materials, Philadelphia, 1985, pp. 282-297.
11. Hooper, S.J., "Tension/Torsional Loading of Composite Laminates with Free-Edge Boundary Conditions", presented at the American Helicopter Society Specialists' Meeting, Williamsburg, VA, October 29, 1991.

**Table I**

Tension Edge Delamination Results

Number of plies	Number of Specimens	Average Critical Strain	Average Modulus, 10 <sup>6</sup> psi	Average Critical load, lb
16	3	0.0060	7.98	3667
32	4	0.0045	7.57	5640

**Table II**

Torsion Edge Delamination Results

Number of plies	Number of specimens	Average gauge length L, in	Average Thickness, in.	Average critical angle per length, $\theta_c/L$ , degrees/in	Average critical torque, $T_c$ , in-lbs.
16	4	3.9	0.0830	5.32	65
16	4	8.3	0.0808	5.35	61
32	4	3.9	0.1670	1.95	162
32	4	8.3	0.1751	2.06	191

**Table III**  
Torsion Crack Angles

Plies	Gauge Length, in.	Angle, degrees		
		Min	Max	Average
16	10	37.1	55.5	49.2
16	5	47.0	56.5	52.0
avg				50.6
32	10	41.0	65.0	49.4
32	5	40.0	64.0	53.8
avg				51.6
				<u>51.1</u>

**Table IV**  
Tension/Torsion Crack Angles

Plies	Gauge Length, in.	Angle, degrees		
		Min	Max	Average
16	10	30	70	48.0
16	5	51	71	57.8
avg				52.9
32	10	33	69	54.9
32	5	24	58	48.3
avg				51.6
				<u>52.2</u>

**TABLE V**  
**AS4/3501-6 GRAPHITE EPOXY**  
**LAMINA PROPERTIES**

$$E_{11} = 19.5 \times 10^6 \text{ Psi}$$

$$E_{22} = 1.48 \times 10^6 \text{ Psi}$$

$$G_{12} = 0.8 \times 10^6 \text{ Psi}$$

$$\nu_{12} = 0.3$$

$$h = 0.005 \text{ in. (ply thickness)}$$

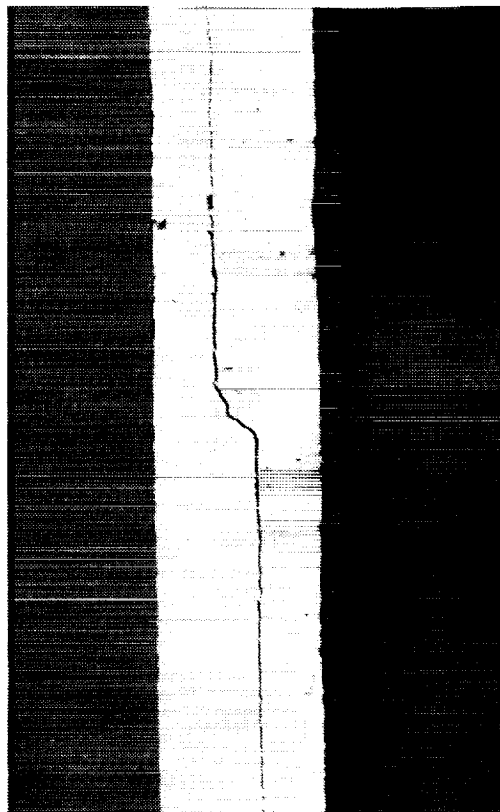


Fig. 1. Photograph of edge of failed specimen showing pattern of cracking in brittle white coating

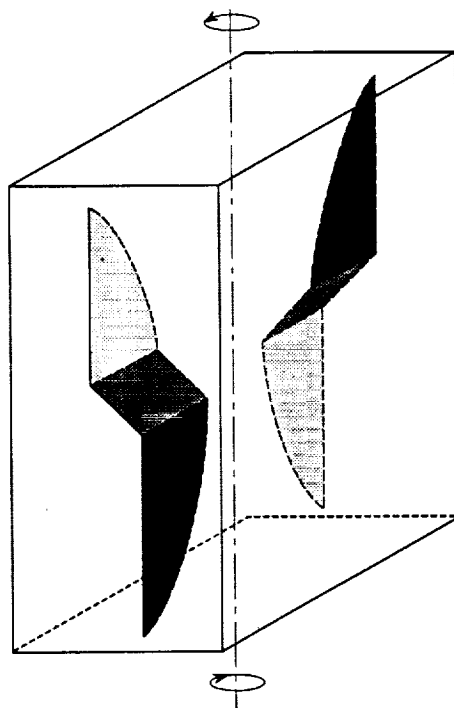


Fig. 2. Schematic of torsion failure mode

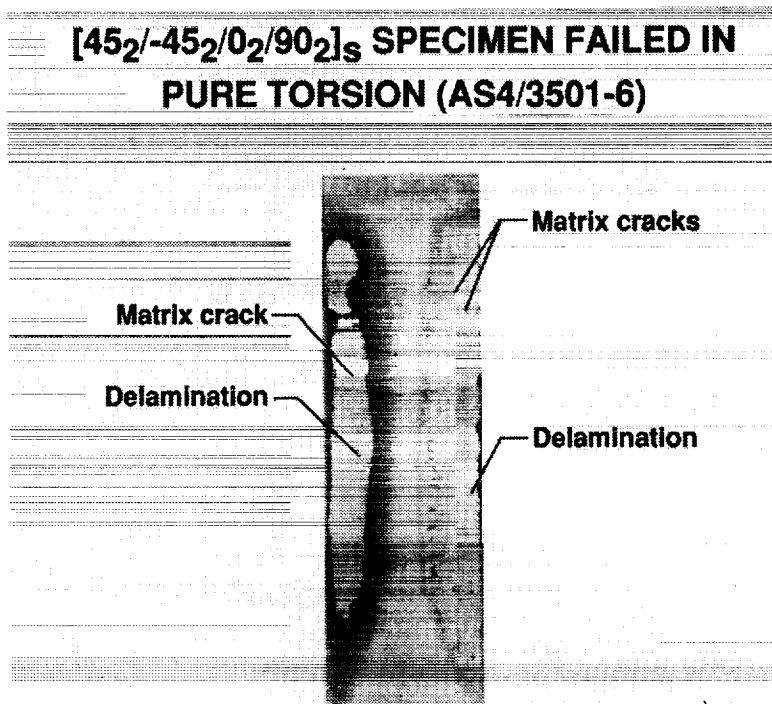


Fig. 3. Dye/penetrant enhanced x-ray radiograph of failed specimen, showing delaminations and ply cracks

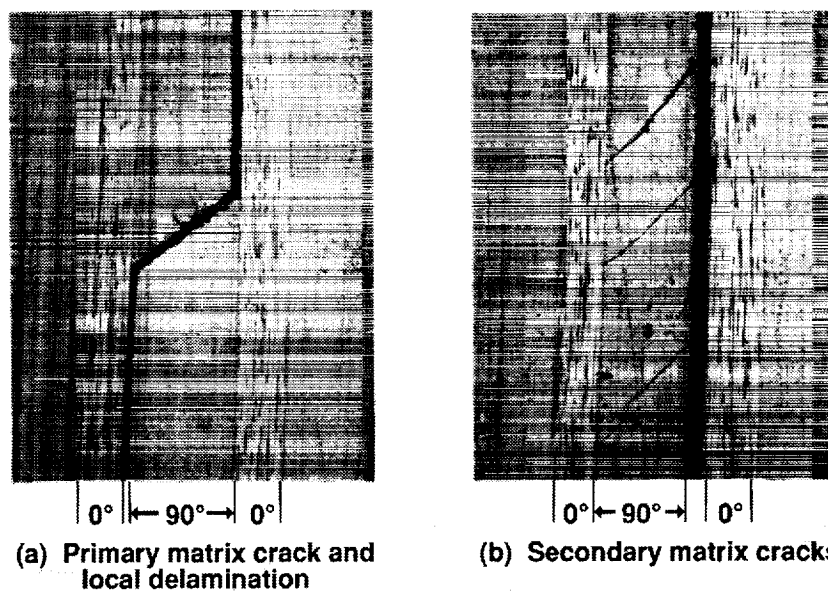


Fig. 4. Optical micrographs of polished edge of 16-ply specimen failed in pure torsion

- a) Primary crack, with delaminations growing from both ends in opposite directions
- b) Secondary cracks and adjacent single delamination

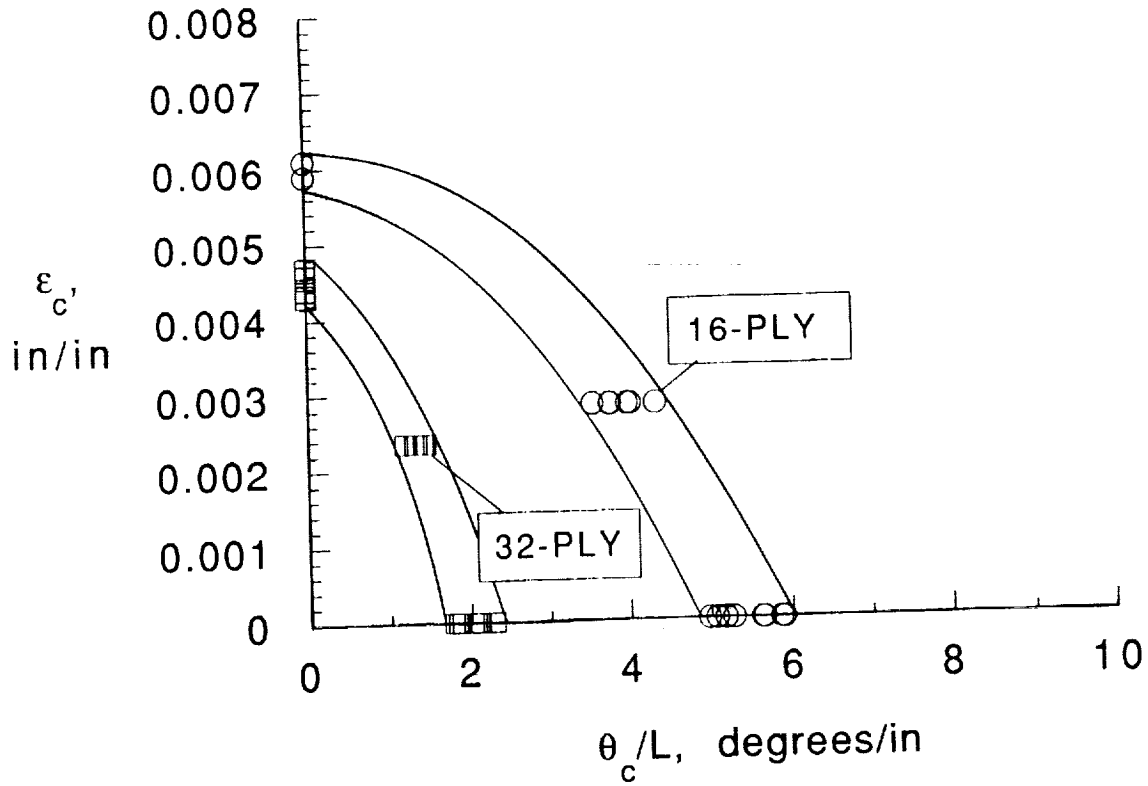


Fig. 5. Combined tension/torsion data plotted as critical axial strain vs. critical angle of twist

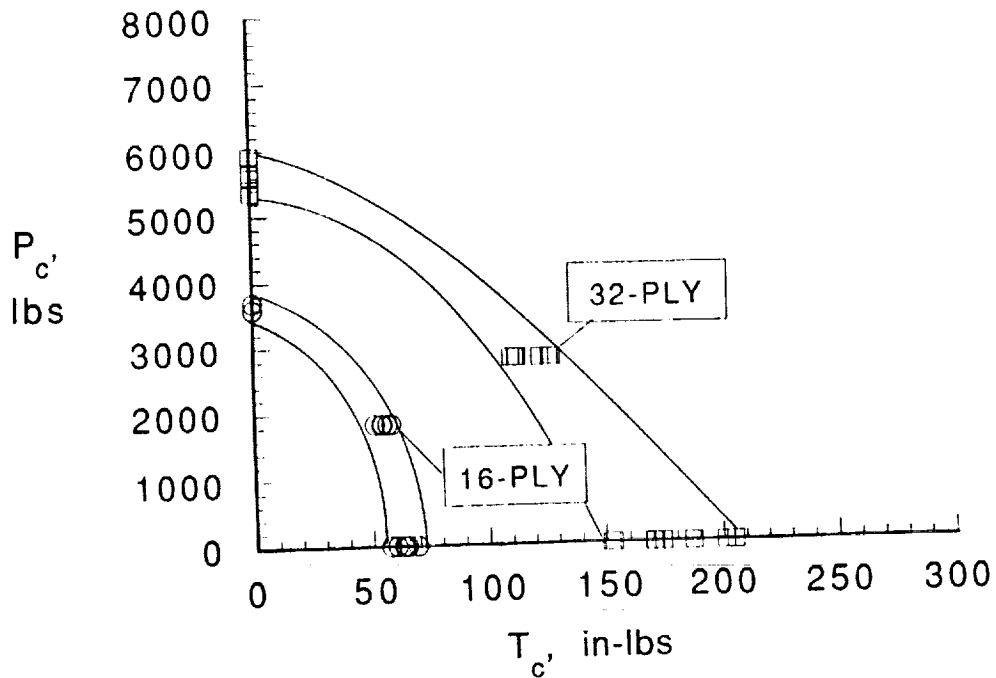


Fig. 6. Combined tension/torsion data plotted as critical axial load vs. critical torque



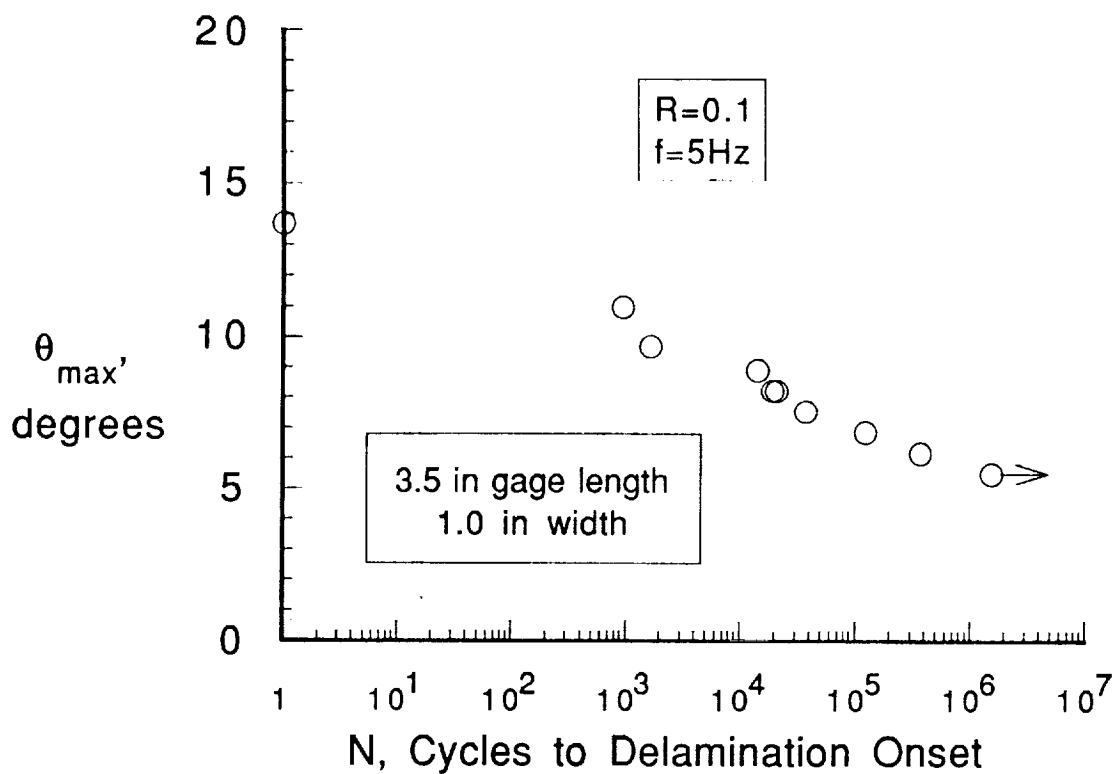


Fig. 7. Critical Torsion angle as a function of number of fatigue cycles

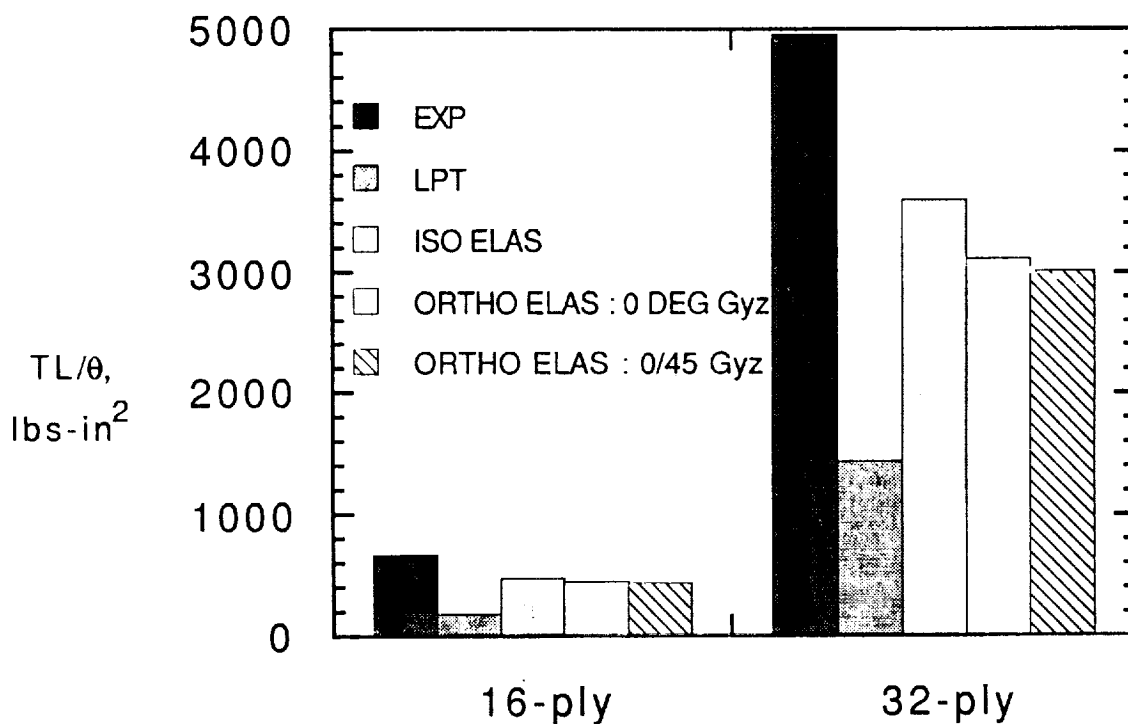


Fig. 8. Measured and calculated torsional rigidities (as described in text)

REPORT DOCUMENTATION PAGE			Form Approved OMB No 0704-0188	
<small>Public reporting burden for this collection of information is estimated to average 7 hours per response, including the time for reviewing instructions, searching existing data sources, gathering and maintaining the data needed, and completing and reviewing the collection of information. Send comments regarding this burden estimate or any other aspect of this collection of information, including suggestions for reducing this burden, to Washington Headquarters Services, Directorate for Information Operations and Reports, 1215 Jefferson Davis Highway, Suite 1204, Arlington, VA 22202-4302, and to the Office of Management and Budget, Paperwork Reduction Project (0704-0188), Washington, DC 20503</small>				
1. AGENCY USE ONLY (Leave blank)	2. REPORT DATE January 1992	3. REPORT TYPE AND DATES COVERED Technical Memorandum		
4. TITLE AND SUBTITLE Delamination Behavior of Quasi-Isotropic Graphite Epoxy Laminates Subjected to Tension and Torsion Loads			5. FUNDING NUMBERS WU 505-63-50	
6. AUTHOR(S) J. A. Hinkley and T. K. O'Brien				
7. PERFORMING ORGANIZATION NAME(S) AND ADDRESS(ES) NASA Langley Research Center and Aerostructures Directorate, USAARTA-AVSCOM, Hampton, VA 23665-5225			8. PERFORMING ORGANIZATION REPORT NUMBER	
9. SPONSORING / MONITORING AGENCY NAME(S) AND ADDRESS(ES) National Aeronautics and Space Administration Washington, DC 20546-0001 and U. S. Army Aviation Systems Command St. Louis, MO 63120-1798			10. SPONSORING / MONITORING AGENCY REPORT NUMBER NASA TM-104181 AVSCOM TR-91-B-018	
11. SUPPLEMENTARY NOTES Hinkley, NASA Langley Research Center, Hampton, VA O'Brien: Aerostructures Directorate, USAARTA-AVSCOM, LaRC Use of trade names or manufacturers in this report does not constitute an official endorsement either expressed or implied by the National Aeronautics and Space Administration.				
12a. DISTRIBUTION / AVAILABILITY STATEMENT Unclassified-Unlimited Subject Category 27			12b. DISTRIBUTION CODE	
13. ABSTRACT (Maximum 200 words) Sixteen and thirty-two ply quasi-isotropic laminates fabricated from AS4-3501-6 were subjected to pure tension, pure torsion, simultaneous tension and torsion, and torsion fatigue. Layups tested were $[45_n/-45_n/0_n/90_n]_s$ , with $n=2$ or $4$ . A torsion damage pattern consisting of a localized matrix crack and delaminations was characterized, and the measured torsional stiffnesses were compared with calculated values. It was found that a combination of tension and torsion led to failure at smaller loads than either type of deformation acting alone. Further work is required to determine the exact form of the failure criterion.				
14. SUBJECT TERMS Graphite-epoxy composites, interlaminar fracture, edge delamination, torsion fatigue cracking			15. NUMBER OF PAGES 16	
			16. PRICE CODE A03	
17. SECURITY CLASSIFICATION Unclassified	18. SECURITY CLASSIFICATION Unclassified	19. SECURITY CLASSIFICATION Of Unclassified	20. LIMITATION OF ABSTRACT	